^{1}H NMR of Aβ Amyloid Peptide Congeners in Water Solution. Conformational Changes Correlate with Plaque Competence†

Jonathan P. Lee,‡,§ Evelyn R. Stimson,‡ Joseph R. Ghilardi,|| Patrick W. Mantyh,|| Yi-An Lu,⊥ Arthur M. Felix,⊥ William Llanos,# Ali Behbin,# Mike Cummings,# Mark Van Criekinge,# William Timms,▽ and John E. Maggio*,‡

Department of Biological Chemistry and Molecular Pharmacology, Harvard Medical School, 240 Longwood Avenue, Boston, Massachusetts 02115, Veteran's Administration Medical Center and Department of Psychiatry, University of Minnesota, Minneapolis, Minnesota 55417, Roche Research Center, Hoffmann-La Roche Inc., Nutley, New Jersey 07110, Research & Development, NMR Instruments, Varian Associates Inc., Palo Alto, California 94304, and Oxford Instruments, Abington Road, Oxford, UK

Received November 23, 1994; Revised Manuscript Received January 27, 1995⊗

ABSTRACT: To begin to examine the structural basis for the deposition of soluble Aβ amyloid peptide onto senile plaques in Alzheimer's disease, we have prepared Aβ congeners and measured their activity in an *in vitro* plaque growth assay. The N-terminal fragment, Aβ(1-28)-OH, was inactive at all pH values tested. While the central fragment, Aβ(10-35)-NH_2, and the full length peptide, Aβ(1-40)-OH, were inactive below pH 4, both were active (plaque competent) between pH 5 and 9. The active and inactive fragments were studied by nuclear magnetic resonance spectroscopy in water at submillimolar concentrations at pH 2.1 and 5.6. Changes in chemical shifts, coupling constants, and nuclear Overhauser enhancements indicate a pH dependent folding transition in Aβ(10-35)-NH_2 as it becomes active. The conformation of the active fragment is not helical, and preliminary data indicate the presence of several turns and at least two short strands. In contrast, the inactive fragment Aβ(1-28)-OH did not undergo a similar folding transition. Earlier nuclear magnetic resonance studies of amyloid peptides in fluorinated alcohols or detergent micelles at low pH described a helical conformation and proposed a helix to sheet transition in plaque formation; the present study demonstrates that no such conformations are present in water under conditions where the peptides can adhere to authentic amyloid plaques.

The pathological hallmark of Alzheimer's disease (AD)[1] is the presence of amyloid plaques surrounded by dead and dying neurons in the brain tissue of victims (Alzheimer, 1907). The principal constituent of AD plaques is the human β-amyloid peptide (Aβ), a 39−43 amino acid peptide of known primary sequence (Roher et al., 1993; Glenner & Wong 1984). The peptide, which is found in normal human tissue (Seubert et al., 1992; Shoji et al., 1992), is derived from a larger protein precursor (Selkoe, 1991). A great deal of circumstantial evidence supporting a central role for Aβ in AD pathology (Selkoe, 1994) has recently been buttressed by the discovery of naturally occurring mutations within Aβ that are linked to the accelerated formation of cerebral amyloid and the early onset of AD (Mullan & Crawford, 1993). More than a dozen other human disorders have also been found to be characterized by the formation of insoluble aggregates composed of naturally occurring proteins (Sipe, 1992). Despite enormous research efforts over the past several years, little high-resolution structural information has been obtained about either the soluble monomeric building blocks or insoluble oligomeric amyloids characterizing these amyloidoses.

What might appear to be a simple problem in the study of a molecular phase transition between a solution and a solid has been complicated by significant technical limitations. A suitable animal model for AD does not exist, and consequently specific residues that are either important or unimportant to plaque formation have been difficult to identify. Many reports have identified either specific residues or segments of Aβ that affect the solubility of the peptide in the micromolar to millimolar concentration range (Hilbich et al., 1991, 1992; Burdick et al., 1992; Dyrks et al., 1993; Jarrett et al., 1993; Castano et al., 1986; Kirschner et al., 1987). However, Aβ is found at sub-nanomolar concentrations (Seubert et al., 1992; Shoji et al., 1992) in human CSF. Furthermore, it is not necessarily true that there is a direct and reliable correlation between *in vitro* insolubility and *in vivo* plaque growth. To address these issues, an assay that measures the deposition of physiological concentrations of Aβ onto authentic AD plaques in human tissue has recently been reported (Maggio et al., 1992).

While clearly of interest, the high-resolution structural features of Aβ (and most other amyloid-forming peptides) are unknown. High-resolution structural studies via either X-ray crystallography or nuclear magnetic resonance (NMR)

† This research was supported by grants to J.E.M. from the National Institutes of Health (GM-15904), the American Health Assistance Foundation, and Hoffmann-La Roche. Work in Oxford, UK, was supported by Varian Associates and Oxford Instruments.

‡ Harvard Medical School.

§ Current address: Department of Chemistry, Boston University, 590 Commonwealth Ave., Boston, MA 02215.

|| University of Minnesota.

⊥ Hoffmann-La Roche, Inc.

Varian Associates Inc.

▽ Oxford Instruments.

⊗ Abstract published in *Advance ACS Abstracts,* March 15, 1995.

[1] Abbreviations: NMR, nuclear magnetic resonance; AD, Alzheimer's disease; CSF, cerebrospinal fluid; SDS, sodium dodecyl sulfate; Ci/mmol, Curie per millimole; PFG, pulsed field gradient; kHz, kilohertz; TSP, trimethylsilyl propionate; TPPI, time proportional phase incrementation; WGS, waveform gradient suppression; NOESY, nuclear Overhauser effect spectroscopy; DQF, double quantum filtered; COSY, correlation spectroscopy; TOCSY, total correlation spectroscopy; MHz, megahertz.

0006-2960/95/0434-5191$09.00/0

spectroscopy have been generally unsuccessful because of the high tendency of Aβ to rapidly form insoluble fibrils. High-resolution structural studies using NMR have been performed upon arbitrarily chosen N-terminal or C-terminal fragments of Aβ under nonphysiological conditions (Barrow & Zagorski, 1991; Spencer et al., 1991; Zagorski & Barrow, 1992; Talafous et al., 1994). The N-terminal 28 residue fragment was studied in 60% trifluoroethanol or 0.45 M sodium dodecyl sulfate (SDS) at low pH and was found to adopt a helical conformation under these conditions (Zagorski et al., 1992; Talafous et al., 1994). The C-terminal fragment was studied as an amorphous solid and is reported to contain an unusual *cis*-peptide bond (Spenser et al., 1991).

In the present study, we have used the plaque growth assay to identify both plaque incompetent and plaque competent fragments of Aβ that are amenable to high-resolution NMR studies in water. ^{1}H NMR data have been acquired for plaque incompetent Aβ(1-28)-OH and plaque competent Aβ-(10-35)-NH_2. Because both fragments of Aβ are inactive at low pH (<4), yet are functionally distinct at pH 5.6, we have used NMR as a probe for detecting changes in the secondary structure of the peptides under conditions that support and do not support plaque growth. This work offers a significant step toward the development of a structure–function model for Aβ deposition onto amyloid plaques in AD.

MATERIALS AND METHODS

Synthetic Peptides, Radioiodination, and Plaque Growth Assay. Peptides were purchased or prepared by the Merrifield solid phase methodology (Barany & Merrifield, 1980), using the fluoren-9-ylmethoxycarbonyl (Fmoc)/*tert*-butyloxycarbonyl (Boc) strategy (Meienhofer et al., 1979). After cleavage from the resin, the crude peptides were purified to homogeneity (>98%) by preparative high-performance liquid chromatography and gave the expected amino acid composition after acid hydrolysis. Further proof of structure was obtained by fast atom bombardment mass spectrometry. After radiolabeling and purification (Too & Maggio, 1991) to a specific activity of 2000 Ci/mmol, ^{125}I-labeled Aβ peptides were applied to brain sections of AD frontal cortex for 2 h as described (Maggio et al. 1992). The peptides were applied at the same concentration (10^{-10} M) and specific activity and labeled at the same amino acid (Tyr 10). Deposition was linear for >24 h, and essentially no deposition was seen in age-matched normal brain tissue. Under these conditions, deposition reflects the binding of soluble monomeric Aβ to amyloid plaque, rather than binding to saturable receptors. Exposure times for autoradiography were identical. Autoradiograms were quantitated by densitometry. The rates of deposition of Aβ(1-42)-OH and Aβ(1-40)-OH were not significantly different under these conditions (J. E. Maggio, unpublished results). A more complete structure–activity profile for Aβ fragments and analogs will be published elsewhere.

NMR Sample Preparation. Dry peptide samples were dissolved in 3 mL of either 90% H_2O/10% D_2O or 60% aqueous trifluoroethanol-d_3, containing 0.5 mM TSP and 0.1 mM NaN_3. The pH (direct meter reading) was adjusted with aqueous HCl or NaOD, and the final volume was adjusted to 3.5 mL. Samples were centrifuged and transferred to 10 mm NMR tubes. Samples were found to be stable for several months at 4 °C.

NMR Spectroscopy. ^{1}H NMR data were collected on a prototype Varian UNITY*plus* 750 MHz NMR machine located at Oxford Instruments (Oxford, U.K.). A prototype 10 mm ^{1}H pulsed field gradient (PFG) probe capable of gradients of >35 G/cm was used for all data collection. Data were collected with a sweep width of 10 kHz using either 16 384 or 8192 complex points for one-dimensional or two-dimensional spectra, respectively, with a relaxation delay of 1.5 s. The beginning of the relaxation delay was preceded by a purging sequence comprising a 1 ms gradient of 5 G/cm, a 90° pulse, and a second 1 ms gradient of 13.5 G/cm. Time domain data were zero filled to double the original size in all dimensions, and digital resolution in the acquisition dimension was 0.6 and 1.2 Hz/pt for one-dimensional and two-dimensional spectra, respectively. All data were acquired at 10 °C. Chemical shifts were referenced to internal TSP at 0.00 ppm. Phase sensitive two-dimensional data sets were acquired using the TPPI–States method (Marion et al., 1989) and >512 complex points were acquired in t_1. Waveform gradient suppression NOESY (WGS-NOESY) spectra were acquired using a standard 64-step phase cycle (unless otherwise specified) with a composite 180° pulse in the middle of the mixing period. Gradients on either side of the composite 180° pulse in the mixing delay were used to enhance solvent suppression and suppress artifacts from multiple quantum coherence. A WGS read pulse module (Figure 1) was substituted for the final 90° pulse in the NOESY experiments, and the module was phase cycled in the standard manner. The gradient strength for the WGS read pulse module was ≤10 G/cm, and the gradients were of 1 ms duration. A gradient recovery delay of 0.5 ms was used to minimize distortions close to the diagonal of the NOESY spectrum. NOESY spectra were acquired using 32 or 64 transients and mixing times of 75 and 150 ms. WGS-TOCSY spectra were acquired using a *z*-filtered, clean DIPSI-2 mixing sequence (Cavanagh & Rance, 1992). Additionally, 1 ms gradients (≤3 G/cm) were included on either side of the mixing sequence, while the magnetization was aligned along the *z*-axis. The total time for the clean DIPSI-2 sequence was ≤77 ms, and a B_1 field strength of ~12 kHz was used for the mixing pulses. Again a WGS read pulse module was substituted for the final 90° pulse and cycled according to Cavanaugh and Rance (1992). PFG-DQF-COSY were acquired as described (Carpenter et al., 1992). All processing and plotting was accomplished using VNMR4.3 software. Using these methods for solvent suppression with the 10 mm ^{1}H PFG probe, the receiver gain could be set approximately 25–35 dB higher than in comparable sequences relying upon solvent pre-irradiation for suppression of the H_2O resonance. The solvent suppression was adequate to allow adjustment of the receiver gain based upon the intensity of the signals of interest rather than spurious voltage arising from an incompletely suppressed H_2O resonance.

RESULTS

Comparison of the Relative Plaque Competence of the Aβ Fragments Aβ(1-28)-OH and Aβ(10-35)-NH_2. Radioiodinated peptides at 0.1 nM concentrations were used to determine the rates of deposition of both [^{125}I]-Aβ(1-28)-OH and [^{125}I]-Aβ(10-35)-NH_2 toward authentic AD plaques relative to [^{125}I]-Aβ(1-40)-OH the major form found in human cerebrospinal fluid (Seubert et al., 1992). At pH 2.1

Table 1: Binding of Aβ-Related Peptides to Authentic AD Plaque

	pH value	
	2.1	5.6
Aβ(1-28)	<1%	<1%
Aβ(10-35)-NH_2	<1%	~37%[a]

[a] Relative to Aβ(1-40) at pH 5.6.

there was no detectable deposition of any of the peptides onto AD plaques (Table 1). In addition, [^{125}I]-Aβ(1-28)-OH was inactive at all pH values measured within the range of 2−11 (data not shown). Because [^{125}I]-Aβ(1-28)-OH remained inactive (less than 0.2% of the activity of [^{125}I]-Aβ(1-40)-OH) toward authentic AD plaques, it has been defined as plaque incompetent. In contradistinction, at pH 5.6, [^{125}I]-Aβ(10-35)-NH_2 demonstrated ~37% activity (relative to the rate of deposition observed for [^{125}I]-Aβ(1-40)-OH at pH 5.6). It is therefore concluded that neither the first nine residues nor the last five residues of Aβ(1-40)-OH are necessary for supporting plaque growth. Moreover, the data indicate that [^{125}I]-Aβ(10-35)-NH_2 contains sufficient structural information to support specific high-affinity deposition onto authentic AD plaques.

Because the plaque competence of [^{125}I]-Aβ(1-40)-OH was similarly pH dependent, and because in our hands [^{125}I]-Aβ(10-35)-NH_2 was found to be more soluble than full length Aβ, we chose the shorter peptide fragment for the development of a model system for structural studies of the pH dependent plaque competence of Aβ peptides. Samples (500 μM) of Aβ(1-28)-OH and Aβ(10-35)-NH_2 at pH 2.1 were prepared for NMR analysis. Identical samples for study at pH 5.6 were also initially prepared at pH 2.1 before the pH was adjusted to 5.6. As the pH was raised toward the isoelectric point of either of the two fragments, the solubility of both samples decreased and some material was lost through flocculant precipitation. Centrifugation was sufficient to remove the insoluble material, and subsequent precipitation was not observed for several months. Both samples of Aβ fragments were considered to be near saturation at pH 5.6. Under these conditions, both samples gave NMR spectra of similar intensity and quality, and amino acid analysis indicated the concentrations of both peptides to be within the range of 250−300 μM. While the decrease in relative solubility for the fragments was similar as the pH was raised from 2.1 to 5.6, the behavior of their respective activities in plaque deposition was very different as the pH was raised from 2.1 to 5.6. This clearly demonstrates that the solubility behavior of synthetic Aβ peptides at concentrations much higher than physiological does not necessarily correlate with their competency in deposition onto AD plaques at physiological concentrations.

^{1}H NMR Assignment of Aβ Congeners at pH 2.1 and 5.6 in Water. To overcome relatively low solubility and the resulting low sensitivity, we took advantage of a prototype 750 MHz NMR machine equipped with ultra-high-performance room temperature shims and a prototype 10 mm ^{1}H PFG probe. The large diameter NMR probe and higher magnetic field afforded approximately 2.5−3 times greater sensitivity than that obtained with similar sample concentrations using a conventional 5 mm ^{1}H probe with pulsed field gradients operating at 500 MHz (data not shown). Because of the higher sensitivity of this prototype NMR system, and because the sample volume was ~7 times greater than in a conventional 5 mm ^{1}H probe, the task of solvent suppression was significantly more demanding. The solvent suppression technique used for all TOCSY and NOESY experiments relied upon substituting the read pulse with a modular pulse sequence element referred to as WGS (waveform gradient suppression) just prior to acquisition (Figure 1). The WGS read pulse module comprises a nonselective 90° pulse followed by a selective gradient refocused echo and results in spectra with essentially no residual signal from water and extremely good phase stability across the entire ^{1}H spectral window. Spectra had only minor distortions arising from relatively small residual DC voltages within the receiver as a result of the large transverse water magnetization just prior to the gradient defocusing and subsequent data acquisition. A 400 μs selective 180° pulse, symmetrically located between the two identical gradients, was tailored for two ±2500 Hz off-resonance excitation maxima. The digital resolution of this doubly shifted pulse was calculated to 200 ns increments, and the excitation maxima were calculated to maintain a constant phase across the entire spectral window. Using the WGS read pulse module, an effective null is realized on resonance and therefore transverse water is defocused by the combined net effect of the two identical gradients. Application of several variations of this type of pulse has recently been described as shifted laminar pulses (Patt, 1992), S pulses, and SS pulses (Smallcombe, 1993).

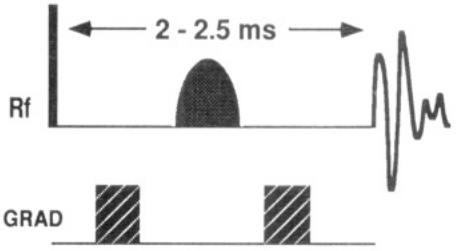

FIGURE 1: Waveform gradient suppression (WGS) pulse sequence module. The phase of both the nonselective 90° pulse and both excitation lobes of the shaped 180° selective pulse are kept identical, and the entire phase of the module is cycled according to the scheme required for the read pulse that is replaced by the module. The selective pulse is equivalent to a 180° SS pulse (Smallcombe, 1993).

A complete set of NMR spectra for both Aβ(1-28)-OH and Aβ(10-35)-NH_2 was measured at pH 2.1 and 5.6 at 10 °C. The assignment of spin systems was completed in a straightforward manner using data from WGS-TOCSY and PFG-DQF-COSY spectra, and sequence specific assignments were made using WGS-NOESY data analyzed using standard methods (Wuthrich, 1986). Representative data from the WGS-TOCSY and WGS-NOESY spectra of Aβ(10-35)-NH_2 are shown in Figures 2 and 3. The assignment data are summarized in Tables S1 and S2 of the supplementary material. The ^{1}H assignment of Aβ(1-28)-OH was completed at both pH values, except for some of the side chain resonances of Lys 16, Lys 28, Arg 5, and Leu 17, as well as all of Asp 1. The unassigned resonances of these spin systems were not accounted for in any of the two-dimensional spectra recorded. This may occur because the signals for these residues either are overlapping with other assigned resonances or are beneath the threshold of detection due to broadening resulting from rotamer exchange on an intermediate time scale. In contrast, with samples of Aβ-(10-35)-NH_2 only the amino resonance of Tyr 10 was unassigned. It is notable that the spin systems for all of the Gly residues within all four samples closely approximated

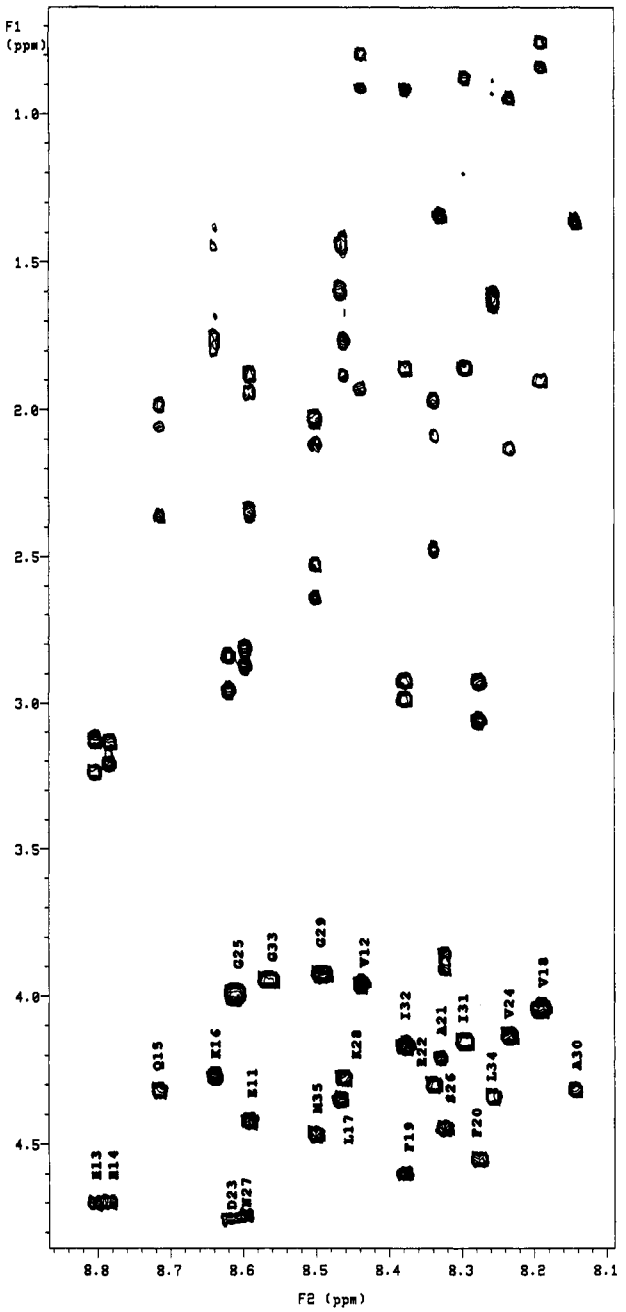

FIGURE 2: Fingerprint region of the TOCSY spectrum of Aβ(10-35)-NH_2 at pH 2.1. Cross peaks between the amide and α-hydrogen atoms of each residue of the peptide are labeled. Each cross peak can be correlated with additional cross peaks dispersed in the F_1 dimension, and nearly all of the spin systems of the peptide can be identified within this expansion.

A_2X patterns (i.e., both α-hydrogen atoms were almost fully degenerate for each individual Gly residue). The chemical shift dispersion of all of the backbone resonances in all samples dissolved in water was relatively modest: ~0.7 ppm for amides and ~0.8 ppm for α-hydrogen atoms. There were no strikingly anomalous chemical shifts, coupling patterns, or evidence of unusually broad line shapes obvious in the one-dimensional survey and two-dimensional correlation spectra.

Chemical Shift Indices of Aβ Fragments. Preliminary analyses of the NMR data to assign patterns of secondary structure for the backbone atoms of the peptides at pH 5.6 relied upon the use of chemical shift indices (CSI) (Wishart et al., 1992). CSI values result from scoring the chemical

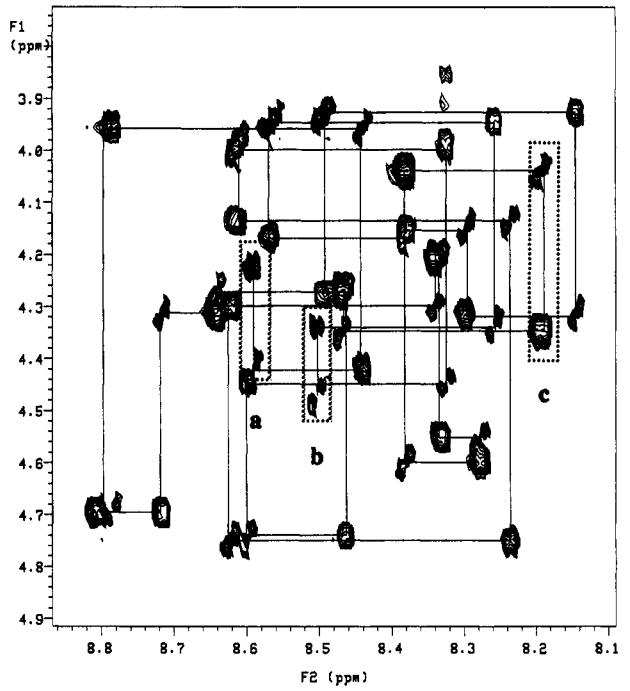

FIGURE 3: Fingerprint region of the NOESY spectrum (mix = 75 ms) of Aβ(10-35)-NH_2 at pH 2.1. Comparison with the same region of Figure 2 allows complete sequential assignment of the entire peptide. The sequential cross peak between the amide and α-hydrogen atoms of Glu 11 and Tyr 10 is shown (box a), as well as those between Met 35 and Leu 34 (box b) and Val 18 and Leu 17 (box c). In this experiment, the phase cycle was reduced to eight steps, and no attempt was made to suppress the antiphase scalar contribution to the intraresidue cross peak. For short mixing times, this produces the observed asymmetric peak shape and becomes an aid in completing sequential assignments in spectra where cross peak degeneracy may occur.

shift of the resonance from the α-hydrogen atoms in polypeptides. Analysis of CSI values (e.g., +1, 0, or −1) can be used to predict the presence of helices, sheets, and turns. CSI analysis of the C-terminus of Aβ(10-35)-NH_2 (residues 29−35; not found within Aβ(1-28)-OH) yielded three values of +1 for the residues Ile 31, Ile 32, and Leu 34 (Figure 4A). The local density of +1 values for the CSI of residues 31−34 is 75%, and there are no −1 values, therefore predicting that, under conditions where Aβ(10-35)-NH_2 is plaque competent, the local conformation of the hydrophobic C-terminus is a short extended strand. Gly 33 gave a CSI value of 0. This value was not judged anomalous by the CSI method for two reasons. The C-terminus is not expected to be found in a highly immobile strand within a multistranded β-sheet, and the absence of a side chain may make a Gly residue in this context mobile enough to appear less structured (recall from earlier that the resonances for α-hydrogen atoms of Gly 33 are nearly degenerate within the NMR spectra). Within the remainder of the peptide (the region common to both Aβ(1-28)-OH and Aβ(10-35)-NH_2), only a single −1 value was found (Glu 11). The majority of the CSI values were determined to be zero, except for the central hydrophobic residues Leu 17, Val 18, and Val 24, where the CSI values were determined to be +1 (Figure 4A).

By using CSI values to predict secondary structure, under conditions where Aβ(10-35)-NH_2 actively adheres to authentic amyloid plaque, there is no evidence supporting the presence of helical regions or multistranded β-sheets. With

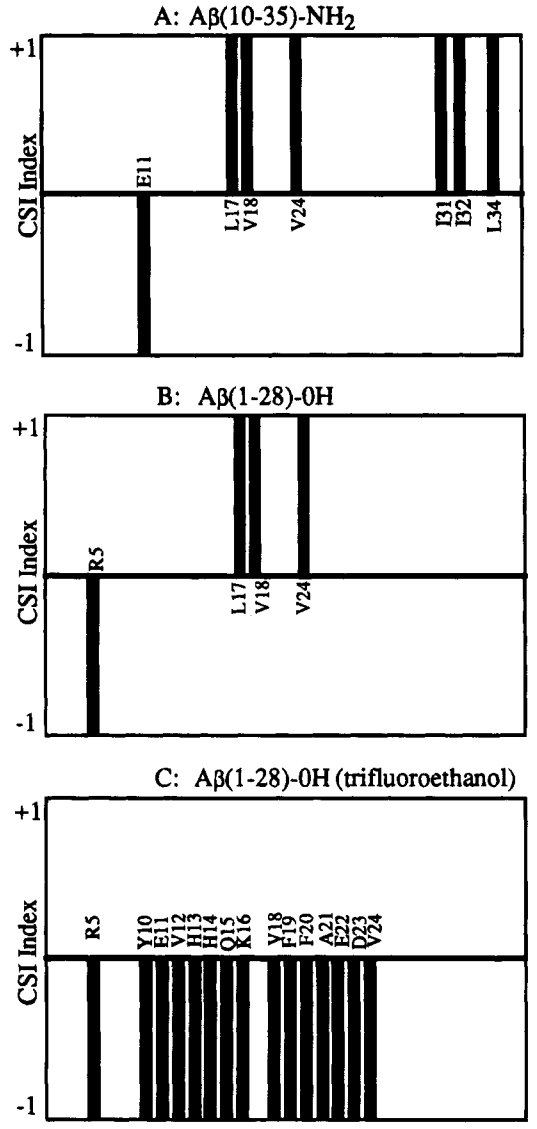

FIGURE 4: (A) CSI results for Aβ(10-35)-NH_2 in water at pH 2.1 and 5.6. (B) CSI results for Aβ(1-28)-OH in water at pH 2.1 and 5.6. (C) CSI results for Aβ(1-28)-OH in 60% trifluoroethanol at pH 3.0. All spectra were scored as described (Wishart et al., 1992).

the exception of a short extended strand within the hydrophobic C-terminus, there is no clear prediction of β-structure. The CSI analysis provides evidence of local structure in the vicinity of the residues with non-zero CSI values, but does not always reveal specific details on the local conformations within these regions. If the hydrophobic C-terminus is maintained in a strandlike structure, then it is anticipated to be stabilized by interstrand hydrogen bonding (Pauling & Corey, 1951) or perhaps hydrophobic interactions. On the basis of CSI analysis of Aβ(10-35)-NH_2, the hydrophobic segment from Leu 17 to Val 24 is the only region that might be predicted to interact with the hydrophobic C-terminus.

CSI analysis of the data for Aβ(1-28)-OH gave a pattern similar to the CSI values for Aβ(10-35)-NH_2 for the region common to both peptides (Figure 4B). With the exception of the absence of the −1 CSI value observed for Glu 11, the pattern within the common region (residues 10−28) of Aβ(1-28)-OH is *identical* to that found for Aβ(10-35)-NH_2. The majority of the residues yield a CSI value of zero, while the same three residues (e.g., Leu 17, Val 18, and Val 24) conspicuously yield CSI values of +1, suggesting that similar local forces dominate the conformation of the backbone of this region. Activity studies further suggest that any local conformation present within this region of Aβ(1-28)-OH is insufficient to confer the ability to adhere to authentic amyloid plaque. The CSI results for the N-terminus of Aβ-(1-28)-OH yielded only a single −1 value for Arg 5, and the remainder of the residues were scored with CSI values of 0. As with plaque competent Aβ(10-35)-NH_2, there is no evidence for the presence of helical regions within Aβ-(1-28)-OH in water. Aside from the central hydrophobic region, from Leu 17 to Val 24, the CSI values predict that the majority of Aβ(1-28)-OH does not have a significant conformational preference under the same conditions where Aβ(10-35)-NH_2 actively adheres to amyloid plaque.

Earlier NMR studies of Aβ(1-28)-OH in fluorinated alcohols (Barrow & Zagorski, 1991; Zagorski & Barrow, 1992) described a helical conformation. Therefore, for comparative CSI evaluation, a complete set of NMR spectra of a 500 μM sample of Aβ(1-28)-OH was also acquired in 60% trifluoroethanol at pH 3.0, conditions reported in the earlier NMR studies (Barrow & Zagorski, 1991; Zagorski & Barrow, 1992). The NMR spectra and the resulting assignments were essentially identical to those previously published for Aβ(1-28)-OH under these conditions. The CSI results for the inactive N-terminal 28-mer in acidic trifluoroethanol are shown in Figure 4C. CSI values of −1 for residues 10−16 and 18−24 are consistent with a peptide of predominantly helical structure. On the basis of CSI analysis, the use of acidic trifluoroethanol as a solvent system significantly stabilizes a helical conformation for the 28-mer. In contrast, the same 28-mer is not predicted to be helical in water. Moreover, the hydrophobic region from Leu 17 to Val 24 is predicted have a conformational preference that is more closely related to an extended strand when Aβ(1-28)-OH is dissolved in water.

Evaluation of $^3J_{HNHa}$ Coupling Constants for Aβ Congeners at pH 2.1 and 5.6. The conformation sensitive (Karplus, 1959) ^3J coupling constants between the amide and α-hydrogen atoms were analyzed for secondary structural elements (Wuthrich, 1986), as well as evidence of pH dependent changes. Values were extracted from one-dimensional spectra, as well as from either high-resolution WGS-TOCSY, WGS-NOESY, or PFG-DQF-COSY data. All of the spectra were characterized by relatively narrow line widths (<3 Hz). The ^3J values obtained were essentially identical regardless of the type of spectrum analyzed or the apodization window applied during processing. Consequently, for the qualitative comparison presented, calculations to correct for line width dependent distortions were not applied. ^3J values for both Aβ(10-35)-NH_2 and Aβ(1-28)-OH at pH 2.1 and 5.6 are presented in Table 2. As the pH is raised from 2.1 to 5.6, acidic residues (Asp and Glu) ionize to carboxylates and His residues become partially deprotonated. These changes in ionization are not anticipated to exert an effect upon the ^3J coupling constants unless there is also a conformational change within the backbone of the peptide. Examination of the ^3J coupling constants for both peptide fragments at pH 2.1 and 5.6 indicates that the pH dependent perturbations can be found primarily within residues located in the region that is common to both Aβ fragments. As the pH is increased, seven ^3J values within the common region are altered by more than 1.5 Hz for the active fragment Aβ(10-35)-NH_2, while only a single ^3J value is similarly altered

Table 2: ^3J Values Determined for Aβ(1-28)-OH and Aβ(10-35)-NH_2[a]

	Aβ(1-28)-OH		Aβ(10-35)-NH_2		
residue	pH 2.1	pH 5.6	pH 2.1	pH 5.6	
Asp 1					
Ala 2	7.8	6.9			
Glu 3	6.6	5.0			
Phe 4	8.3	6.0			
Arg 5	8.3				
His 6	5.2	4.1			
Asp 7	5.0	4.0			
Ser 8	6.3	6.3			
Gly 9					
Tyr 10	8.2	8.1			
Glu 11	7.0	6.3	**7.8**	**4.6**	
Val 12	7.6	7.3	6.6	6.7	
His 13	7.7	7.7	**8.3**	**5.8**	
His 14	6.8	7.7	**8.2**	**5.3**	
Gln 15	7.3	6.3	**5.2**	**3.6**	
Lys 16	6.6	5.8	5.0	4.6	
Leu 17	7.1	7.0	6.3	6.5	
Val 18	7.7	9.0	8.2	8.5	
Phe 19	6.8	8.0	7.0	7.8	
Phe 20	7.5	8.3	7.6	8.2	
Ala 21	5.9	6.7	**7.7**	**4.5**	
Glu 22	**7.7**	**5.8**	**5.8**	**4.2**	
Asp 23	7.3	8.3	**7.3**	**5.4**	
Val 24	6.6	6.0	6.6	5.3	
Gly 25					
Ser 26	7.3	7.6	7.1	6.5	
Asn 27			7.9	7.7	8.0
Lys 28			7.6	4.8	5.5
Gly 29					
Ala 30				5.7	5.9
Ile 31			7.7	7.7	
Ile 32			6.9	7.3	
Gly 33					
Leu 34			6.6	6.4	
Met 35			7.3	7.5	

[a] All values are ±0.6 Hz, and they are uncorrected for line widths. Values in boldface type change by more than 1.5 Hz as the pH is changed.

for the inactive fragment Aβ(1-28)-OH. An increase in the pH decreases the ^3J values for residues within two local segments of Aβ(10-35)-NH_2, from His 13 to Lys 16 and from Ala 21 to Val 24. The ^3J values for the intervening hydrophobic segment, Leu 17−Phe 20, remain relatively large regardless of the pH of the sample or the peptide studied. Collectively the data suggest that a pH dependent folding transition occurs about the conformationally restricted hydrophobic residues within the Leu 17−Phe 20 region of the active fragment Aβ(10-35)-NH_2 and that such a transition is not readily apparent for the inactive fragment Aβ(1-28)-OH. Figure 5 compares the ^3J values for both Aβ fragments at pH 5.6. For active Aβ(10-35)-NH_2, the relatively small ^3J values found in the two regions His 13−Lys 16 and Ala 21−Val 24 are juxtaposed against the relatively large ^3J values for the intervening hydrophobic region Leu 17−Phe 20. As shown in Figure 5, this contrast is not found for Aβ(1-28)-OH. The data suggest that the pH dependent folding transition involves the formation of a turn−strand−turn motif within the three aforementioned regions, extending from His 13 to Val 24.

Evidence That Active Aβ(10-35)-NH_2 Is Folded. Figure 6 compares one-dimensional projections of NOESY spectra for the amide hydrogen atom of Ala 21 in the context of both Aβ(1-28)-OH and Aβ(10-35)-NH_2 at pH 5.6. The NOE correlations between the methyl group of Ala 21 and its

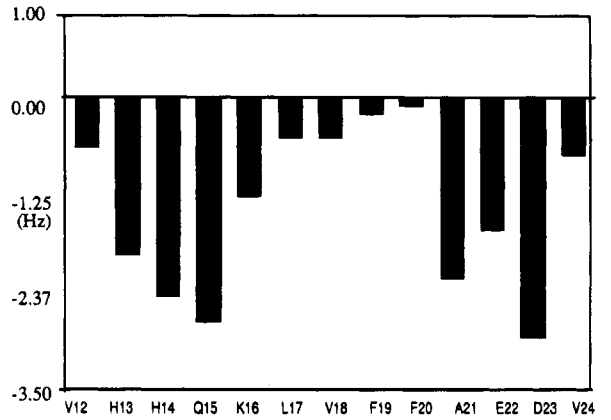

FIGURE 5: Comparison of the net difference in $^3J_{HN-H\alpha}$ for Aβ(10-35)-NH_2 and Aβ(1-28)-OH in water at pH 5.6 for the common region from Val 12 to Val 24 demonstrates the conformational differences for the two identical sequences in the context of an active and an inactive peptide. The relative decrease in the values for the two regions bracketing the central hydrophobic stretch is even more conformationally distinct via computation of the average $^3J_{HN-H\alpha}$ value for Val 18−Phe 20 in Aβ(10-35)-NH_2. This value of 8.2 Hz is used to partially define a central turn−strand−turn conformational motif within Aβ(10-35)-NH_2 under conditions where the fragment is active.

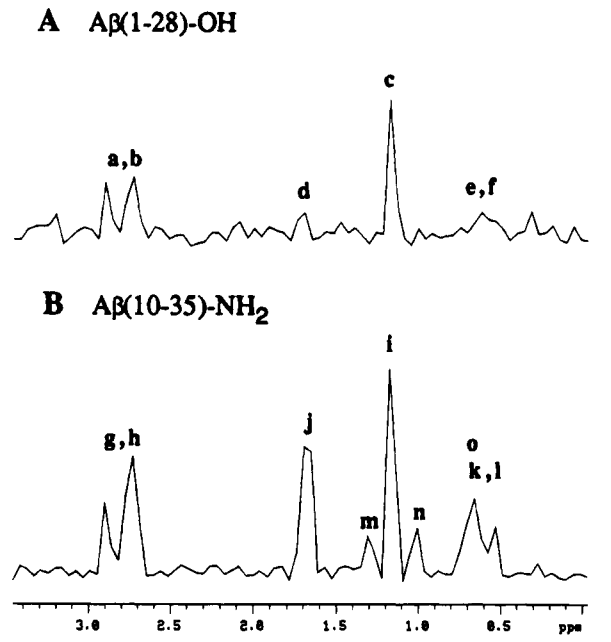

FIGURE 6: Comparison of slices through the two-dimensional NOESY spectra of Aβ(10-35)-NH_2 and Aβ(1-28)-OH in water at pH 5.6 for the signal corresponding to the amide hydrogen atom of Ala 21 in both samples. (Panel A) Peaks a and b arise from the sequential β-methylene signals of the $i-1$ residue (Phe 20); peak c is from the intraresidue methyl group of Ala 21. Peaks d, e, and f are possibly from medium range interactions with the β-methine and two γ-methyl groups of Val 18. (Panel B) Peaks g, h, and i are the same as a, b, and c; peaks j, k, and l can be unambiguously assigned to the β-methine and two γ-methyl groups of Val 18. Peaks m and n have been partially assigned to the γ-methylene group of Ile 31 and/or Ile 32. The increased intensity and additional broadness toward the downfield side of peak k is not consistent with the complementary cross peak in the symmetric quadrant of the NOESY spectrum. Therefore, a tentative partial assignment as peak o, from a C-terminal methyl group (e.g., Ile 31 or Ile 32), is being considered in designing future isotope-filtered experiments. The extreme intensity of peak j is similarly being considered.

amide hydrogen atom, as well as between the β-methylene group of Phe 20 and the amide hydrogen atom of Ala 21,

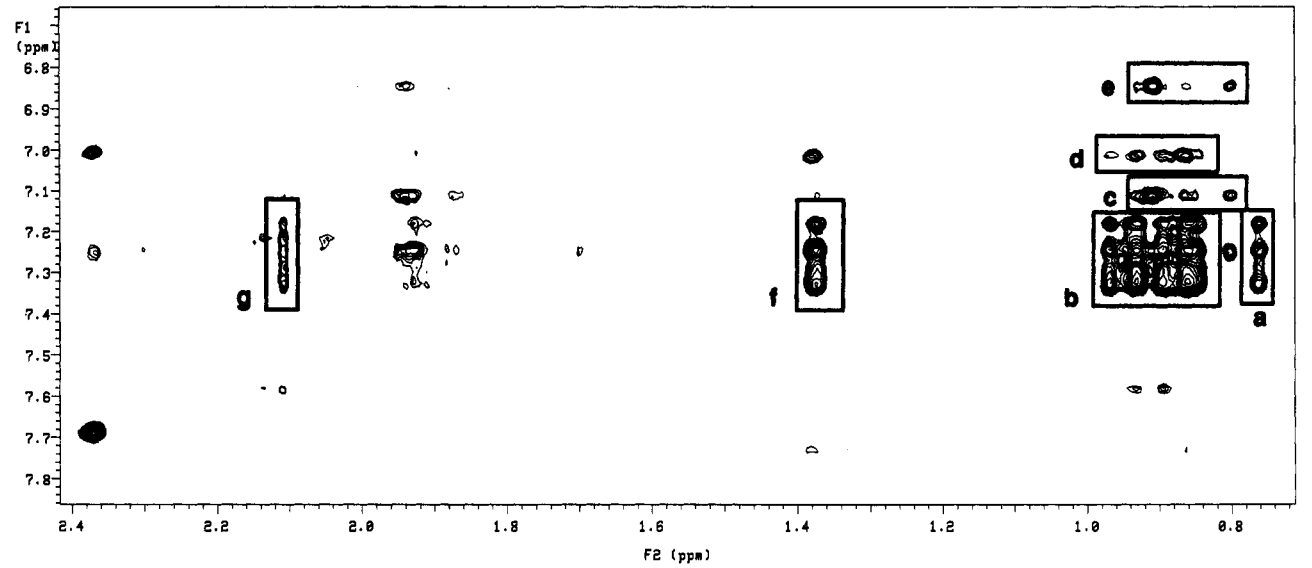

FIGURE 7: Expansion of the NOESY spectrum of Aβ(10-35)-NH_2 in water at pH 5.6. Box **a** shows NOE interactions between the aromatic hydrogen atoms of both Phe 19 and Phe 20 and the γ_2-methyl group of Val 18; box b contains a similar cross peak between the same aromatic groups and the γ_1-methyl group of Val 18, as well as cross peaks from the methyl groups of Leu 17 and other methyl groups that cannot be further assigned using these data. Box c contains cross peaks between the 2,6-positions of Tyr 10 and the γ-methyl groups of Val 12 and also contains an additional weak cross peak at 0.87−0.88 ppm in the F_2 dimension. Because this is the only long range correlation to Tyr 10, and because it may originate from either Val 18, Ile 31, and/or Ile32, a conformational interpretation has been delayed. Box d contains cross peaks between the amide hydrogen atoms of both Gln 15 and Asn 27 and a group of nearly degenerate methyl resonances, which remain unassigned in these data. Box e gives information similar to that of box c but for the 3,5-positions of Tyr 10 and includes the additional weak long range correlation. The cross peaks of box f are between the aromatic hydrogen atoms of both Phe 19 and Phe 20 and the methyl group of Ala 21. Within box g are the long range cross peaks between the aromatic hydrogen atoms of both Phe 19 and Phe 20 and the ϵ-methyl group of Met 35. The narrowness of the cross peak in the F_2 dimension reflects the sharpness of the methyl resonance due to the absence of scalar coupling.

are more intense in the spectrum of the active fragment than in the spectrum of the inactive fragment. In the spectrum of the active fragment there are also several unique NOE correlations between the amide hydrogen atom of Ala 21 and the atoms found in the side chain of Val 18 (medium range), as well as the side chain atoms of Ile 31 (long range). Figure 7 depicts intense NOE cross peaks within the NOESY spectrum of the active fragment between several high-field resonances and the ring systems of Tyr 10, His 13, His 14, Phe 19, and Phe 20. Several of these long range correlations between the methyl groups of the hydrophobic residues at the C-terminus and the aromatic residues within the central hydrophobic region have been assigned. However, because of chemical shift degeneracy, complete assignment of all of the NOE correlations will require the analysis of isotope-edited NOESY data of ^{13}C-, ^{15}N-, and ^{2}H-enriched peptides (J. P. Lee, in progress). NOE correlations between the ϵ-methyl group of Met 35 and the aromatic rings of both Phe 19 and Phe 20 can be assigned (Figure 7), and they provide additional strong evidence that, under conditions where Aβ(10-35)-NH_2 is active, the peptide exists in a folded conformation. Numerous other long range NOE correlations can be found in the spectrum of the active fragment, including weak cross peaks between the H-4 position of an imidazole ring (His 13 or His 14) and the γ-hydrogen atoms of Glu 22 (data not shown). Finally, the presence of a folded conformation for the active fragment Aβ(10-35)-NH_2 juxtaposed against an unfolded conformation for the inactive fragment Aβ(1-28)-OH is supported by comparing the HN−HN region of the NOESY spectra for the two peptides at pH 5.6 (Figure 8). The spectrum of the active peptide shows several short regions of relatively intense sequential NOE cross peaks between amide hydrogen atoms. Corresponding NOE cross peaks in the spectrum of the inactive peptide are significantly weaker or unobservable altogether.

DISCUSSION

Our results indicate that by using the plaque growth assay with synthetic radioiodinated peptides the relative plaque competence of different Aβ congeners can be determined. A particularly salient feature of this assay is the determination of biological activity at peptide concentrations found physiologically. Using the assay, we demonstrate that plaque competence is pH dependent for both Aβ(1-40)-OH and Aβ-(10-35)-NH_2 and that Aβ(1-28)-OH is plaque incompetent at all pH values tested. The assay has allowed us to functionally define three regions in the primary sequence of Aβ with respect to their relative importance for detectable plaque growth. We find the following: (1) the first 28 residues are insufficient to support plaque growth; (2) the first nine residues are unnecessary for supporting plaque growth; and (3) the last five residues are also unnecessary for supporting plaque growth. In functionally defining the truncated fragment Aβ(10-35)-NH_2 as containing both necessary and sufficient information to support highly specific binding to authentic AD plaques, we also define a model peptide system with improved solubility characteristics relative to the full length Aβ peptide. These results simultaneously overcome several technical limitations that have thwarted progress in AD research during the past several years, thereby enabling the structure-based analysis of the relative importance of a broad spectrum of parameters that may or may not be significant for the growth of amyloid plaques in AD.

The plaque competent peptide congener and the plaque incompetent congener have similar molecular weights and

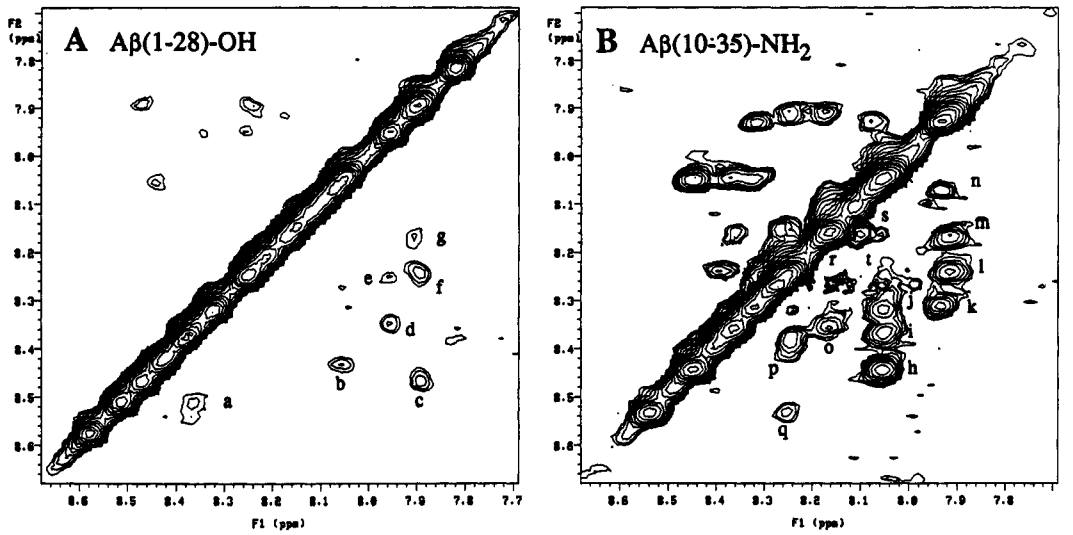

FIGURE 8: NOESY data for Aβ(1-28)-OH and Aβ(10-35)-NH_2 in water at pH 5.6. The connectivities established by the cross peaks in these spectra are from NOE interactions between sequential amide hydrogen atoms. Panel A: cross peaks a (His 6/Asp 7), b (Gly 25/Ser 26), c (Gly 9/Tyr 10), d (His 13/His 14), e (Tyr 10/Glu 11), f (Leu 17/Val 18), and g (Val 18/Phe 19). Panel B: cross peaks h (Val 24/Gly 25), i (Gly 33/Leu 34), j (Asp 23/Val 24), k (Gly 29/Ala 30), l (Leu 17/ Val 18), m (Val 18/Phe 19), n (Ala 30/Ile 31), o (Ile 32/Gly 33), p (Asn 27/Lys 28), q (Val 12/His 13), r (Phe 20/Ala 21), s (Phe 19/Phe 20), and t (Ile 31/Ile 32).

net charges and demonstrated similar characteristic pH dependent insolubility. We therefore provide the first direct evidence that highly specific plaque competence does not necessarily correlate directly with a reduction in peptide solubility. The poor fidelity of such a correlation may be responsible for many of the conflicting reports that have appeared during the past several years, suggesting that different portions of the Aβ peptide may be of more or less importance to the amyloid deposition process that defines Alzheimer's disease. We have found the plaque growth assay to be a powerful and versatile method, and it is possible that this type of assay can be adapted for broad application toward the elucidation of molecular information about other amyloidoses.

Using ^{1}H NMR, we report the sequential assignment and secondary structural analysis of two Aβ fragments in water under conditions where both fragments are inactive, as well as under conditions where the fragment Aβ(10-35)-NH_2 tightly adheres to authentic amyloid plaque. By using CSI analysis (Wishart et al., 1992), the C-terminal strand of Aβ-(10-35)-NH_2 is predicted to exist as a short, extended strand and the remainder of the peptide is neither helix nor sheet. Within the central hydrophobic region, from Leu 17 to Val 24, there is evidence for a conformational predisposition. The stabilization of the C-terminal strand can be expected to occur via interactions with residues that are not located within the same strand. Therefore, on the basis of the CSI approach, it can be reasoned that the conformation of the hydrophobic C-terminus is likely to be stabilized via interactions with the only other conformationally defined region, e.g., the central hydrophobic region. This central region (Leu 17 to Val 24) is also present in plaque incompetent Aβ(1-28)-OH, and the CSI method predicts a similar local conformational predisposition. Because this reasoning is supported by additional NMR data (i.e., ^3J and NOE data), it follows that this local conformational preference exists in both peptides, yet there is insufficient structural information within such a conformational preference to result in plaque competence.

In comparing CSI results under conditions where Aβ(10-35)-NH_2 is either active or inactive, the CSI method does not predict a dramatically different secondary structure. Minor changes in chemical shift were observed for many residues. However, because these changes fall beneath the CSI threshold of ±0.1 ppm, they were judged to be relatively minor. Under conditions where the peptide is inactive, the peptide is therefore likely to be partially folded and could be described as an ensemble of rapidly exchanging forms within the conformational space. By changing conditions to those that support plaque growth, the peptide would become confined to a single conformation, presumably very similar to one of those preexisting within the ensemble. Plaque competence would then be expected to be associated with either a decrease in the energy of a local minimum in the conformational space or, alternatively, an increase in the energy of conformations in close proximity to the local minimum.

Analysis of ^3J coupling constants provided a more sensitive indicator to monitor differences in the conformation of Aβ-(10-35)-NH_2 under conditions where the peptide is either active or inactive. The evidence supports a pH dependent folding transition about a conformationally predisposed hydrophobic region from Leu 17 to Phe 20, corroborating and extending the CSI predictions. Ionizable residues that titrate on either side of this region help form at least two separate turns within the backbone of Aβ(10-35)-NH_2 as it becomes active. The data indicate that the pH dependent folding transition is characterized by the appearance of a turn−strand−turn motif within residues His 13−Val 24. The transition is not observed for the plaque incompetent Aβ-(1-28)-OH. Because this occurs as the Aβ peptide congener attains the ability to adhere to amyloid plaque, this folding transition may therefore define a conformational marker for solution behavior that is consistent with plaque competence.

Further support for a pH dependent folding transition for Aβ(10-35)-NH_2 can be found in our preliminary analysis of

NOESY cross peaks, obtained under conditions where the peptide is plaque competent. As the pH was raised from 2.1 to 5.6, we observed increases in short and medium range internuclear correlations and several new long range correlations between the aromatic rings of Phe 19 (and/or Phe 20) and the methyl groups of the C-terminal residues (Ile 31−Met 35), providing clear evidence of a folded conformation at pH 5.6. In addition, the long range correlations between Glu 22 and His 13 (or His 14) suggest the formation of a salt bridge, presumably adding to the stability of the folded conformation and offering a plausible explanation for the pH dependence of the folding transition. The data therefore indicate that, under conditions where Aβ(10-35)-NH_2 can adhere to authentic amyloid plaque, a solution conformation exists that (i) is stabilized via interactions between hydrophobic residues of a C-terminal strand (Ile 31−Met 35) and a central strand (Leu 17−Phe 20), (ii) is further stabilized by interactions between ionizable residues located on either side of the central hydrophobic strand, and (iii) these ionizable residues are present within turns within the backbone of the peptide that bracket the conformationally predisposed central hydrophobic strand.

Previous ^{1}H NMR studies (Zagorski & Barrow, 1992; Talafous et al., 1994) have suggested the importance of helical structure for the soluble form of Aβ(1-28)-OH, but these studies were not conducted in water. Because poor solubility in water has often been an intractable problem for the study of the solution conformation of peptides by ^{1}H NMR, some researchers have chosen to adopt experimental conditions that include an acidic environment in nonaqueous solvents (e.g., acidic trifluoroethanol or hexafluoroisopropyl alcohol). It is also well-known that such solvent systems can stabilize the formation of nascent helices (Dyson et al., 1988). The use of such solvent systems should only be considered valid within the context of a developing structure−function relationship when strong precedent exists for the normal physiological presence of a helical structure. Our work suggests that this is not the case for the study of Aβ and its congeners. Our data clearly indicate that Aβ(1-28)-OH is inactive at plaque growth and, without acidic trifluoroethanol or other modifiers, gives no indication of a helical conformation in water. The hypothesis of a helix to sheet transition for soluble Aβ (Zagorski & Barrow, 1992) also is not supported by our work. Our data (chemical shifts, coupling constants, and NOEs) clearly indicate that, under conditions where Aβ(10-35)-NH_2 can adhere to authentic amyloid plaque, the peptide is not helical in solution. This work does not preclude the possibility that within a membrane-like environment, as simulated through the use of fluorinated alcohols or SDS within a solvent system, Aβ and its congeners may exist in a helical conformation.

There are at least two features of the conformation of Aβ-(10-35)-NH_2 that are similar to concepts put forth in previous studies. Kirschner et al. (1987) and Fraser et al. (1991) proposed ion paring or electrostatic interactions between histidine residues and carboxylates within the cross-β-structure believed to occur within amyloid plaques. Fraser et al. (1991) and Hilbich et al. (1991) have proposed the importance of interactions involving the hydrophobic region from Leu 17 to Phe 20 for the formation of amyloid plaque. While both of these predictions rely upon chemical concepts that are included in our interpretation of the data presented earlier, there is a fundamental difference in our work. We report results as part of a high-resolution study of the intramolecular interactions within a soluble molecule, rather than inferences concerning the interactions that underlie insoluble fibril formation. The importance of the ionizable amino acid side chains for stabilizing the solution conformation of the soluble form of Aβ(10-35)-NH_2 is shown by the occurrence of a pH dependent folding transition, which can be associated with plaque competence. In addition, the structural predisposition involving the central hydrophobic region, and its role in stabilizing the local conformation of the hydrophobic C-terminal strand, clearly establishes the importance of both hydrophobic regions in stabilizing a folded solution conformation under conditions where Aβ-(10-35)-NH_2 is active. Because the solution conformation under study does not resemble the predicted cross-β-structure believed to occur within amyloid plaques, several issues must be addressed. The identification of several key residues that can be implicated in the stabilization of the solution conformation of Aβ(10-35)-NH_2 under conditions that support plaque growth clearly underscores the potential role of these residues within all aspects of Aβ conformation. This may include conformational changes or conformational stabilization of Aβ within amyloid plaque, or it may relate to potential interactions with other normal physiological constituents.

While it is possible that the solution conformation exists within plaques, it seems more likely that a conformational change must occur within the Aβ peptide during plaque formation. The stabilizing interactions detected within the solution conformation of the active Aβ congener are relatively sparse, as is often the case with relatively short acyclic polypeptides. The sum of these interactions might be expected to be energetically less favorable than the sum of those expected to exist within the predicted cross-β-structure of amyloid plaque. It follows that the Aβ peptide could be energetically perched in a metastable solution conformation. Detailed knowledge of the prerequisites and behavior of this solution conformation should provide essential information in testing this hypothesis, as well as potentially aiding in the development of novel strategies for directing the Aβ peptide into alternative physiological outcomes instead of the formation of amyloid plaque. Therefore, we believe that this work offers a significant step toward defining a useful structure−function model for the soluble component involved in the formation of amyloid plaque in Alzheimer's disease.

ACKNOWLEDGMENT

The authors are grateful for many useful discussions with Gerhard Wagner, Timothy F. Havel, Christopher T. Walsh, Steve Smallcombe, Dan Kirschner, and Stephen P. Watson.

SUPPLEMENTARY MATERIAL AVAILABLE

Tables listing the resonance assignments for Aβ(10-35)-NH_2 and Aβ(1-28)-OH at pH 2.1 and 5.6 (4 pages). Ordering information is given on any current masthead page.

REFERENCES

Alzheimer, A. (1907) *Z. Psychiatry 64*, 146−148.

Barany, G., & Merrifield, R. B. (1980) *The Peptides: Analysis, Synthesis, Biology* (Gross, E., & Meienhofer, J., Eds.) Vol. 2, pp 1−384, Academic, New York.

Barrow, C. J., & Zagorski, M. G. (1991) *Science 253*, 179−182.
Barrow, C. J., Yasuda, A., Kenny, P. T. M., & Zagorski, M. G. (1992) *J. Mol. Biol. 225*, 1075−1093.
Burdick, D., Soreghan, B., Kwon, M., Kosmoski, J., Knauer, M., Henschen, A., Yates, J., Cotman, C., & Glabe, C. (1992) *J. Biol. Chem. 267*, 546−554.
Carpenter, T. A., Colebrook, L. D., Hall, L. D., & Pierens, G. K. (1992) *Mag. Reson. Chem. 30*, 168−773.
Castano, E. M., Ghiso, J., Prelli, F., & Gorevic, P. D., et al. (1986) *Biochem. Biophys. Res. Commun. 141*, 782−789.
Cavanagh, J., & Rance, M. (1992) *J. Magn. Reson. 96*, 670−678.
Dyrks, J. H., Dyrks, E., Masters, C. L., & Beyreuther, K., (1993) *FEBS Lett. 324*, 231−236.
Dyson, H. J., Rance, M., Houghten, R. A., Lerner, R. A., & Wright, P. E. (1988) *J. Mol. Biol. 201*, 201.
Fraser, P. E., Nguyen, J. T., Surewicz, W. K., & Kirschner, D. A. (1991) *Biophys. J. 60*, 1190−1201.
Glenner, G. G., & Wong, C. W. (1984), *Biochem. Biophys. Res. Commun. 120*, 885−890.
Hilbich, C., Kisters-Woike, B., Reed, J., Masters, C. L., & Beyreuther, K. (1991) *J. Mol. Biol. 218*, 149−163.
Hilbich, C., Kisters-Woike, B., Reed, J., Masters, C. L., & Beyreuther, K. (1992) *J. Mol. Biol. 220*, 460−473.
Jarrett, J. T., Berger, E. P., & Lansbury, P. T., Jr. (1993) *Biochemistry 32*, 4693−4697.
Karplus, M. (1959) *J. Phys. Chem. 30*, 11−15.
Kirchner, D. A., Inouye, H., Duffy, L. K., Sinclair, A., Lind, M., & Selkoe, D. J. (1987) *Proc. Natl. Acad. Sci. U.S.A. 84*, 6953−6957.
Maggio, J. E., Stimson, E. R., Ghilardi, J. R., Allen, C. J., Dahl, C. E., Whitcomb, D. C., Vigna, S. R., Vinters, H. V., Labenski, M. E., & Mantyh, P. W. (1992) *Proc. Natl. Acad. Sci. U.S.A. 89*, 5462−5466.
Marion, D., Ikura, M., Tschudin, R., & Bax, A. (1989) *J. Magn. Reson. 85*, 393−399.
Meienhofer, J., Waki, M., Heimer, E. P., Lambros, T. J., Makofske, R. C., & Chang, C.-D. (1979) *Intl. J. Pept. Protein Res. 13*, 35−42.
Mullen, M., & Crawford, F. (1993) *Trends Neurosci. 16*, 398−403.
Patt, S. L. (1992) *J. Magn. Reson. 96*, 94−102.
Pauling, L., & Corey, R. B. (1951) *Proc. Natl. Acad. Sci. U.S.A. 37*, 729−740.
Roher, A. E., Lowenson, J. D., Clarke, S., Woods, A. S., Cotter, R. J., Gowing, E., & Ball, M. J. (1993) *Proc. Natl. Acad. Sci. U.S.A. 90*, 10836−10840.
Selkoe, D. J. (1991) *Neuron 6*, 487−498.
Selkoe, D. J. (1994) *J. Neuropathol. Exp. Neurol. 53*, 438−447.
Seubert, P., Vigo-Pelfrey, C., Esch, F., Lee, M., Dovey, H., Davis, D., Sinha, S., Schossmacher, M., Whaley, J., Swindlehurts, C., McCormack, R., Wolfert, R., Selkoe, D., Lieberburg, I., & Schenk, D. (1992) *Nature 359*, 325−327.
Shoji, M., Golde, T. E., Ghiso, J., Cheung, T. T., Estus, S., Shaffer, L. M., Cai, X.-D., McKay, D. M., Tinter, R., Frangione, B., & Younkin, S. G. (1992) *Science 258*, 126−129.
Sipe, J. D. (1992) *Annu. Rev. Biochem. 61*, 947−975.
Smallcombe, S. (1993) *J. Am. Chem. Soc. 115*, 4776−4785.
Spencer, R. G., Halverson, K. J., Auger, M., McDermott, A. E., Griffen, R. G., & Lansbury, P. T., Jr. (1991) *Biochemistry 30*, 10382−10387.
Talafous, J., Marcinowski, K. J., Klopman, G., & Zagorski, M. G. (1994) *Biochemistry 33*, 7788−7796.
Too, H.-P., & Maggio, J. E. (1991) *Methods Neurosci. 6*, 232−247.
Wishart, D. S., Sykes, B. D., & Richards, F. M. (1992) *Biochemistry 31*, 1647−1651.
Wuthrich, K. (1986) *NMR of Proteins and Nucleic Acids*, Wiley-Interscience, New York.
Zagorski, M. G., & Barrow, C. J. (1992) *Biochemistry 31*, 5621−5631.

BI9427126